Migrations of the Carbon Atom of the $SC(H)PR_3$ Ligand in the Reduction/Protonation Processes of Heterodinuclear Mn−Re Complexes†

Daniel Miguel*

Departamento de Química Inorgánica, Facultad de Ciencias, Universidad de Valladolid, C/ Prado de la Magdalena s/n, E-47071 Valladolid, Spain

Jing Li,‡ Dolores Morales, and Víctor Riera

Departamento de Química Orgánica e Inorgánica/IUQOEM-Unidad Asociada del CSIC, Universidad de Oviedo, E-33071 Oviedo, Spain

Santiago García-Granda

Departamento de Química Física y Analítica, Universidad de Oviedo, 33071 Oviedo, Spain

Received January 12, 2001

The reaction of $[MnRe(CO)_6(\mu\text{-}S_2CPR_3)]$ (R = Cy (**1a**), Pr^i (**1b**)) with Na[Hg] in THF affords anionic species which, after protonation with excess NH_4PF_6, produce neutral $[MnRe(CO)_6(\mu\text{-}SH)\{\mu\text{-}SC(H)PR_3\}(NH_3)]$ (**3a**,**b**). These are unstable and rapidly isomerize, at room temperature, to more stable complexes **4a**,**b**. The NH_3 ligand can be replaced in **3** and **4** by better donors such as PEt_3 or $NCBu^t$, affording derivatives $[MnRe(CO)_6(\mu\text{-}SH)\{\mu\text{-}SC(H)PR_3\}(L)]$, which are isostructural respectively to **3a**,**b** (complexes **5a**−**d**) and to **4a**,**b** (complexes **6a**−**d**). The structures of these two series have been confirmed by X-ray crystallographic studies on derivatives **5a** (R = Cy, L = PEt_3) and **6d** (R = Pr^i, L = $CNBu^t$). A detailed examination of the structures reveals that both series of isomers contain the bridging ligands SH and $SC(H)PR_3$, which have been produced by the cleavage of a C−S bond during the reduction/protonation process which involves also the cleavage of the metal−metal bond. All this parallels the behavior previously observed for their homobinuclear dimanganese and dirhenium analogues. A remarkable novel feature that appears in the heterobinuclear Mn/Re system is that the central carbon of S_2CPR_3, which was bonded to Mn in the starting **1a**,**b**, is bonded to Re in complexes **3**, after the C−S splitting, and ends up bonded again to Mn in complexes **4**. Thus, the reduction/protonation/isomerization sequence involves two migrations of the carbon atom: first from Mn to Re and then back from Re to Mn. In light of the structural and spectroscopic data available, it can be assumed that the driving force behind these migrations is of electronic rather than steric nature, and several paths for the process are proposed and discussed.

Introduction

The chemistry of heterobinuclear complexes has been a very active field of research in the past decades. It is expected that the selective reactivity arising from the combination of two different metals could be exploited in useful applications such as homogeneous catalysis or transition metal mediated organic synthesis.[1] The formation of M−C bonds, while constituting the central core of organometallic chemistry, remains the key step in many useful catalytic and stoicheiometric reactions of organic substrates. Although a great amount of work has been done, much remains to be known in order to understand the factors governing the formation of metal-to-carbon bonds, especially when two different metals are present. Previous studies on complexes containing S_2CPR_3 bridges have revealed that the central carbon atom of the ligand is able to discriminate between two different metal atoms, exhibiting a clear preference for one of them.[2] More recently we have shown that the reduction and subsequent protonation of homobinuclear $[M_2(CO)_6(\mu\text{-}S_2CPR_3)]$ (M = Mn, Re) complexes occur with cleavage of the M−M and one S−C bond of S_2CPR_3, to afford complexes incorporating the two resulting fragments: SH^- and $SC(H)PR_3^-$, as bridges between the metals.[3]

† Dedicated to Professor Rafael Usón on the occasion of his 75th birthday.

* Corresponding author. Tel: int+34 983 423232. Fax: int+34 983 423013. E-mail: dmsj@qi.uva.es.

‡ Present address: Institute of Elemento-Organic Chemistry, Nankai University, 300071 Tianjin, China.

(1) Roberts, D. A.; Geoffroy, G. L. In *Comprehensive Organometallic Chemistry;* Wilkinson, G., Stone, F. G. A., Abel, E. W., Eds.; Pergamon Press: Oxford, U.K., 1982; Chapter 40.

(2) For a discussion on this point and leading references see: Galindo, A.; Miguel, D.; Pérez, J. *Coord. Chem. Rev.* **1999**, *193*−*195*, 643.

(3) Li, J.; Miguel, D.; Morales, M. D.; Riera, V.; García-Granda, S. *Organometallics* **1998**, *17*, 3448.

10.1021/om0100232 CCC: $20.00
Publication on Web 06/15/2001

Scheme 1

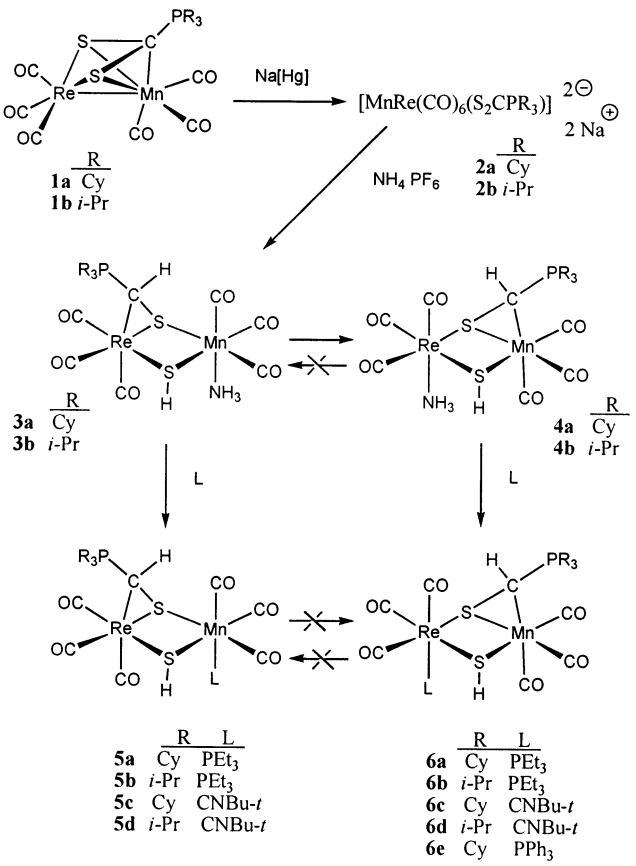

In this paper we present the extension of this chemistry to heterobinuclear Mn−Re substrates. As with their homobinuclear analogues, the reduction/protonation sequence produces the cleavage of the Mn−Re bond and one C−S bond. Additionally, we have observed a remarkable succession of two processes of irreversible migration of the carbon atom of the ligand $SC(H)PR_3$ from Mn to Re and back to Mn. These can be interpreted on the basis of the different electronic conditions on the metal atoms.

Results and Discussion

Treatment of cooled (0 °C) THF solutions of heterobinuclear $[MnRe(CO)_6(\mu\text{-}S_2CPR_3)]$ (**1a**,**b** in Scheme 1) with excess 1% sodium amalgam for 15 min gave orange-red solutions, which exhibited IR spectra consisting of four bands at frequencies much lower than those of the starting compounds. This is consistent with the formation of carbonyl anions **2a**,**b** (see Scheme 1) and parallels the behavior of the homonuclear dimanganese and dirhenium analogues.[3]

When solutions of **2a**,**b** are transferred onto solid NH_4PF_6, protonation occurs instantaneously, as judged from IR monitoring: the bands of anions **2a**,**b** are replaced by a set of six new bands shifted to higher frequencies, attributable to complexes **3a**,**b**. On standing in solution at room temperature for several minutes, compounds **3a**,**b** are transformed into new complexes **4a**,**b**, with IR spectra consisting of a new set of four ν(CO) bands with frequencies and relative intensities significantly different from those of **3a**,**b**. The same transformation from **3** to **4** is produced if the solution of **3** is evaporated to dryness and the solid redissolved in THF. Apparently, the protonation of anions **2a**,**b** affords initially the kinetic complexes **3a**,**b**, which are readily transformed into the thermodynamically more stable species **4a**,**b**. Complexes **3a**,**b**, therefore, could not be isolated, while **4a**,**b** were obtained as microcrystalline solids and fully characterized by analytical and spectroscopic methods. The structures depicted for complexes **3** and **4** in Scheme 1 are proposed on the basis of the available spectroscopic data, together with the structural determinations of one derivative of each series as described below.

Despite their instability, freshly prepared solutions of **3a**,**b** can be used in situ to obtain derivatives $[MnRe(CO)_6(\mu\text{-}SH)\{\mu\text{-}SC(H)PR_3\}(L)]$ (**5a**,**b** in Scheme 1) by substitution reactions with PEt_3 or $CNBu^t$. It is necessary to carry out the reactions at low temperature, by mixing the reactants at −78 °C, to minimize the isomerization from **3** to **4**. The resulting derivatives **5a**−**d** were isolated as stable crystalline solids and were characterized by analytical and spectroscopic methods (see Experimental Section).

The availability of complexes of type **5** is limited by the properties of the entering ligands. Thus, when a bulky and less nucleophilic phosphine, such as PPh_3, is used, the reaction does not proceed at low temperature, and some warming is necessary. In such conditions it is not possible to avoid the isomerization from **3** to **4** and the subsequent substitution gives a complex of type **6** (**6e** in Scheme 1, see below for explanation).

The IR solution spectra of **5a**−**d** exhibit ν(CO) bands with the same pattern and with frequencies very close to those observed for **3a**,**b**, suggesting that both series of complexes have similar structures, and, therefore, the structural determination of one of the derivatives would serve to indirectly characterize complexes **3a**,**b.** To ascertain the geometry of these complexes, an X-ray determination was carried out on a crystal of derivative **5a** (L = PEt_3). A perspective view is presented in Figure 1, crystal and refinement details are in Table 1, and selected bond distances and angles are in Table 2.

The structure of **5a** is similar to that found for the dirhenium analogue $[Re_2(CO)_6(\mu\text{-}SH)\{\mu\text{-}SC(H)PCy_3\}(NH_3)]$.[3] The fragments $Mn(CO)_3$ and $Re(CO)_3$ are bridged by the groups hydrogensulfide, SH^-, and *trialkylphosphoniothiolateylide*, $SC(H)PR_3^-$, which come from the splitting of S_2CPR_3. The Mn···Re distance of 3.772(1) Å is too long to permit any significant interaction between the two metals. The trialkylphosphoniothiolateylide is bonded as η^1-(S) to manganese [Mn−S(1) 2.416(3) Å] and η^2-(S,C) to rhenium [Re−S(1) 2.463(4) Å, Re−C(1) 2.221(1) Å]. As occurred with their homobinuclear Mn_2 and Re_2 congeners, the reduction/protonation sequence involves the cleavage of the Mn−Re and one of the C−S bonds. However, the most remarkable feature of the structure of **5a** is that the central carbon of the $SC(H)PR_3$ ligand is bonded to Re, while it was bonded to Mn in the parent compound. Since IR data suggest that complexes **5a**−**d** are isostructural to **3a**,**b**, it is apparent that, in addition to the C−S cleavage, the reduction/protonation process leading from **1** to **3** involves the migration of the central carbon from Mn to Re. This point will be discussed below with some detail.

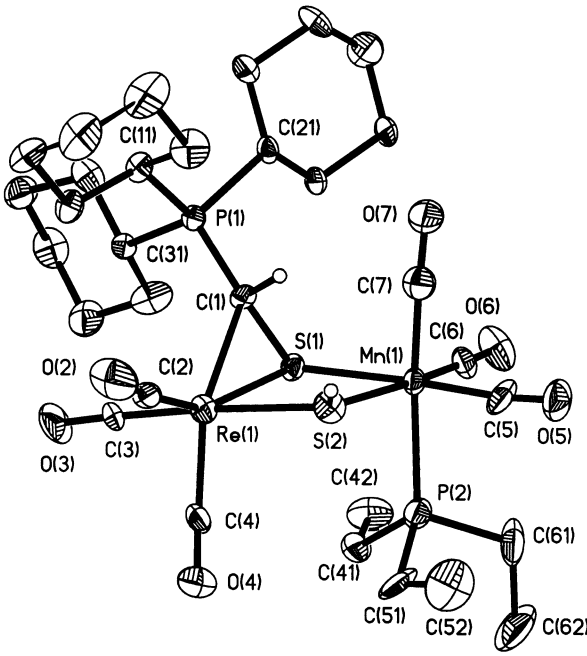

Figure 1. Perspective view of the molecule of $[MnRe(CO)_6(\mu\text{-}SH)\{\mu\text{-}SC(H)PCy_3\}(PEt_3)]$ (**5a**), showing the atom numbering.

Table 1. Crystal Data and Refinement Details for $[MnRe(CO)_6\{\mu\text{-}SC(H)PCy_3\}(\mu\text{-}SH)(PEt_3)]$ (5a) and $[MnRe(CO)_6\{\mu\text{-}SC(H)PPr^i_3\}(\mu\text{-}SH)(CNBu^t)]$ (6d)

	5a	**6d**
formula	$C_{31}H_{50}MnO_6P_2ReS_2$	$C_{21}H_{32}MnNO_6PReS_2$
fw	885.94	730.72
cryst system	orthorhombic	monoclinic
space group	*Pcab* (No. 61)	$P2_1/c$ (No. 14)
a, Å	18.481(6)	18.239(5)
b, Å	18.776(4)	10.766(2)
c, Å	21.980(4)	15.869(3)
β, deg	90	115.40(2)
V, Å^3	7627(3)	2815(1)
Z	8	4
T, K	293	293
ρ_{calc}, g cm^{-3}	1.54	1.72
F(000)	3568	1440
λ (Mo Kα), Å	0.71069	0.71069
cryst size, mm; color	0.2 × 0.1 × 0.1, yellow	0.3 × 0.2 × 0.2, orange
μ, cm^{-1}	37.56	50.18
method of collection	$\omega/2\theta$ scan	$\omega/2\theta$ scan
scan range, deg	$1 \le \theta \le 25$	$1 \le \theta \le 25$
abs corr	semiempirical (ψ-scan)	
correction factors (min., max.)	0.844, 1.000	0.856, 1.000
no. of reflns measd	7806	5440
no. of reflns unique	6692	4947
no. of reflns obsd, $I = 3\sigma(I)$	3725	3798
weighting scheme	$w = [\sigma^2(F) + gF^2]^{-1}$	
g	0.00010	0.00011
no. of params	397	316
residuals *R*, wR_2	0.0717, 0.2584	0.0259, 0.0685

Ammonia complexes **4a**,**b** react with PEt_3 or $CNBu^t$ to afford stable crystalline complexes $[MnRe(CO)_6(\mu\text{-}SH)\{\mu\text{-}SC(H)PR_3\}(L)]$ (**6a**−**e** in Scheme 1). A crystal of **6d** (L = $CNBu^t$) was subjected to an X-ray structural detemination. The results are presented in Table 1 (crystal and refinement data), Figure 2 (perspective view), and Table 3 (selected bond lengths and angles)

The molecule of **6d** consist of two fragments, $Re(CO)_3$ and $Mn(CO)_3$, which are held together by SH^- and $SC(H)PR_3^-$ bridges, the two metals being too far apart [Mn(1)···Re(1) 3.772(1) Å] to sustain any interaction. In general, the geometrical parameters are close to those found for **5a** (compare Table 2 and Table 3). However, there is a major difference: the phosphoniothiolateylide is now bonded as η^2-(C,S) to Mn [Mn(1)−C(1) 2.073 Å, Mn(1)−S(1) 2.3507(13) Å] and as η^1-(S) to Re. Accordingly, the entering ligand L (*tert*-butylisocyanide in the

Table 2. Selected Interatomic Distances (Å) and Angles (deg) in $[MnRe(CO)_6\{\mu\text{-}SC(H)PCy_3\}(\mu\text{-}SH)(PEt_3)]$ (5a)

Re(1)−S(1)	2.463(4)	Re(1)−S(2)	2.530(4)
Re(1)−C(2)	1.82(2)	Re(1)−C(3)	1.872(17)
Re(1)−C(4)	1.930(16)	Re(1)−C(1)	2.221(12)
Mn(1)−S(1)	2.416(3)	Mn(1)−S(2)	2.443(5)
Mn(1)−C(6)	1.750(18)	Mn(1)−C(7)	1.780(17)
Mn(1)−C(5)	1.807(16)	Mn(1)−P(2)	2.374(4)
S(1)−C(1)	1.786(13)	C(1)−P(1)	1.780(11)
C(2)−O(2)	1.25(2)	C(3)−O(3)	1.17(2)
C(4)−O(4)	1.119(19)	C(5)−O(5)	1.141(18)
C(6)−O(6)	1.196(19)	C(7)−O(7)	1.187(19)
C(2)−Re(1)−C(3)	89.5(8)	C(2)−Re(1)−C(4)	91.5(7)
C(3)−Re(1)−C(4)	86.7(6)	C(2)−Re(1)−C(1)	110.3(6)
C(3)−Re(1)−C(1)	97.9(6)	C(4)−Re(1)−C(1)	157.7(6)
C(2)−Re(1)−S(1)	153.7(5)	C(3)−Re(1)−S(1)	100.0(5)
C(4)−Re(1)−S(1)	113.3(5)	C(1)−Re(1)−S(1)	44.5(3)
C(2)−Re(1)−S(2)	93.6(7)	C(3)−Re(1)−S(2)	176.0(5)
C(4)−Re(1)−S(2)	90.7(5)	C(1)−Re(1)−S(2)	83.4(3)
S(1)−Re(1)−S(2)	78.28(12)	C(6)−Mn(1)−C(7)	91.2(7)
C(6)−Mn(1)−C(5)	91.9(8)	C(7)−Mn(1)−C(5)	87.7(7)
C(6)−Mn(1)−P(2)	88.7(5)	C(7)−Mn(1)−P(2)	174.9(5)
C(5)−Mn(1)−P(2)	87.2(5)	C(6)−Mn(1)−S(1)	91.9(5)
C(7)−Mn(1)−S(1)	94.3(5)	C(5)−Mn(1)−S(1)	175.6(6)
P(2)−Mn(1)−S(1)	90.82(13)	C(6)−Mn(1)−S(2)	172.8(5)
C(7)−Mn(1)−S(2)	90.0(6)	C(5)−Mn(1)−S(2)	95.2(6)
P(2)−Mn(1)−S(2)	90.75(16)	S(1)−Mn(1)−S(2)	80.90(13)
C(1)−S(1)−Mn(1)	103.9(4)	C(1)−S(1)−Re(1)	60.6(4)
Mn(1)−S(1)−Re(1)	101.28(13)	Mn(1)−S(2)−Re(1)	98.65(14)
P(1)−C(1)−S(1)	122.1(7)	P(1)−C(1)−Re(1)	132.2(7)
S(1)−C(1)−Re(1)	75.0(4)	O(2)−C(2)−Re(1)	172.7(16)
O(3)−C(3)−Re(1)	176.9(15)	O(4)−C(4)−Re(1)	176.6(17)
O(5)−C(5)−Mn(1)	174.1(16)	O(6)−C(6)−Mn(1)	177.9(16)
O(7)−C(7)−Mn(1)	175.7(16)		

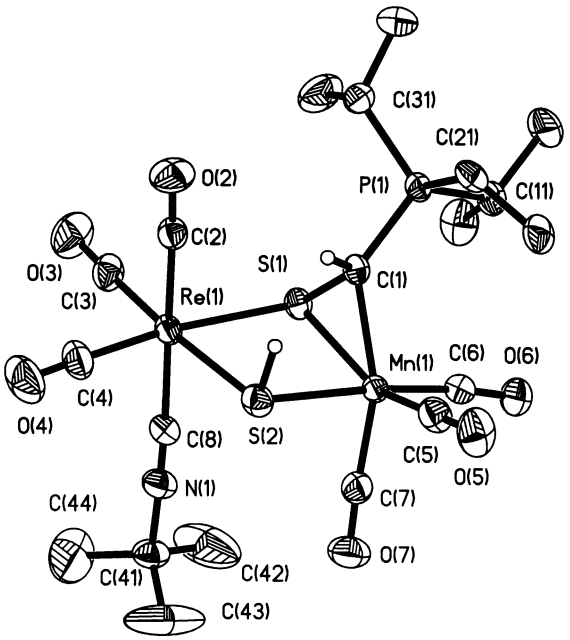

Figure 2. Perspective view of the molecule of $[MnRe(CO)_6(\mu\text{-}SH)\{\mu\text{-}SC(H)PCy_3\}(CNBu^t)]$ (**6d**), showing the atom numbering.

Table 3. Selected Interatomic Distances (Å) and Angles (deg) in [MnRe(CO)$_6${μ-SC(H)PPr$^i_3$}(μ-SH)(CNBu^t)] (6d)

Re(1)−C(4)	1.901(6)	Re(1)−C(3)	1.908(6)
Re(1)−C(2)	1.944(5)	Re(1)−C(8)	2.088(5)
Re(1)−S(1)	2.5016(12)	Re(1)−S(2)	2.5282(14)
Mn(1)−C(5)	1.776(5)	Mn(1)−C(6)	1.780(5)
Mn(1)−C(7)	1.793(5)	Mn(1)−C(1)	2.073(5)
Mn(1)−S(1)	2.3507(13)	Mn(1)−S(2)	2.4520(14)
S(1)−C(1)	1.788(4)	C(1)−P(1)	1.782(4)
C(2)−O(2)	1.129(6)	C(3)−O(3)	1.142(6)
C(4)−O(4)	1.146(6)	C(5)−O(5)	1.165(6)
C(6)−O(6)	1.154(6)	C(7)−O(7)	1.151(6)
C(8)−N(1)	1.146(6)		
C(4)−Re(1)−C(3)	91.8(2)	C(4)−Re(1)−C(2)	90.1(2)
C(3)−Re(1)−C(2)	86.3(2)	C(4)−Re(1)−C(8)	91.8(2)
C(3)−Re(1)−C(8)	91.7(2)	C(2)−Re(1)−C(8)	177.33(19)
C(4)−Re(1)−S(1)	171.64(19)	C(3)−Re(1)−S(1)	96.42(17)
C(2)−Re(1)−S(1)	91.98(14)	C(8)−Re(1)−S(1)	86.46(13)
C(4)−Re(1)−S(2)	92.60(19)	C(3)−Re(1)−S(2)	175.55(17)
C(2)−Re(1)−S(2)	92.92(14)	C(8)−Re(1)−S(2)	88.91(14)
S(1)−Re(1)−S(2)	79.21(4)	C(5)−Mn(1)−C(6)	88.2(2)
C(5)−Mn(1)−C(7)	94.8(2)	C(6)−Mn(1)−C(7)	88.9(2)
C(5)−Mn(1)−C(1)	108.0(2)	C(6)−Mn(1)−C(1)	98.7(2)
C(7)−Mn(1)−C(1)	156.10(19)	C(5)−Mn(1)−S(1)	154.88(19)
C(6)−Mn(1)−S(1)	98.59(16)	C(7)−Mn(1)−S(1)	109.43(16)
C(1)−Mn(1)−S(1)	47.16(12)	C(5)−Mn(1)−S(2)	91.49(18)
C(6)−Mn(1)−S(2)	175.01(16)	C(7)−Mn(1)−S(2)	86.14(16)
C(1)−Mn(1)−S(2)	86.17(13)	S(1)−Mn(1)−S(2)	83.74(5)
C(1)−S(1)−Mn(1)	58.24(15)	C(1)−S(1)−Re(1)	103.87(15)
Mn(1)−S(1)−Re(1)	99.39(5)	Mn(1)−S(2)−Re(1)	96.01(5)
P(1)−C(1)−S(1)	120.0(2)	P(1)−C(1)−Mn(1)	133.1(2)
S(1)−C(1)−Mn(1)	74.59(17)	O(2)−C(2)−Re(1)	175.8(4)
O(3)−C(3)−Re(1)	176.7(5)	O(4)−C(4)−Re(1)	177.3(6)
O(5)−C(5)−Mn(1)	178.1(5)	O(6)−C(6)−Mn(1)	173.1(5)
O(7)−C(7)−Mn(1)	176.8(5)	N(1)−C(8)−Re(1)	176.5(4)
C(8)−N(1)−C(41)	177.3(5)		

case of **6d**) is now bonded to rhenium instead of manganese. The comparison of the IR spectra for complexes **4** and **6** does not help very much to assign the geometry for the series **4a**,**b**. While complexes **6a**−**d** (and also **3a**,**b** and **5a**−**d**) exhibit a pattern of six bands, complexes **4** display a unique pattern of only four bands, probably due to some accidental degeneracy. Nevertheless the comparison of the ^{13}C NMR spectra is more informative: for the series with SC(H)PCy$_3$, the signal of the carbon bonded to Re appears at δ around 20 ppm (20.5 for **5a**, 19.4 for **5c**), while when the carbon atom is bonded to Mn, the signal is shifted to higher frequencies and appears consistently at around δ 30 ppm (29.8 for **4a**, 31.9 for **6a**, and 31.2 for **6c**). This, together with other spectroscopic features, strongly suggests that derivatives **6a**−**d** are isostructural to their parent compounds **4a**,**b.** Thus, the isomerization of complexes **3** to give **4** involves the migration of the carbon atom of the SC(H)PR$_3$ ligand from Re to Mn, which is accompanied by the complementary migration of the ammonia ligand in the opposite direction, from Mn to Re.

Attempting to get additional information, we carried out the protonation of the anion **2** in the presence of excess NH$_3$ by transferring the solution of **2** onto solid NH$_4$PF$_6$ while a current of NH$_3$ gas was bubbled through the solution. Under these conditions, the formation of complex **3** was virtually instantaneous, as it was in the absence of excess NH$_3$. However, complex **3** could be kept for 4 h under NH$_3$ without any significant isomerization to **4**. It must be recalled that, in the absence of NH$_3$, **3** is transformed into **4** within several minutes.

On the other hand, if the solvent THF is replaced by CH$_2$Cl$_2$, the isomerization is completed within minutes, even under excess NH$_3$, to give **4**, which is stable in solution for several hours. In the absence of excess NH$_3$, the solution of **4** in CH$_2$Cl$_2$ undergoes extensive decomposition within 1 h. All these facts point out that the presence of a coordination vacancy is needed to produce the isomerization from **3** to **4**. Additionally, derivatives **5** or **6**, which contain nonlabile ligands such as PEt$_3$ or CNBu^t, do not isomerize at room temperature or even after several hours under reflux.

It has been shown above that the reduction/protonation process leading from **1** to **3** involves the migration of the central carbon of the S$_2$CPR$_3$ ligand from Mn to Re, whereas in the subsequent isomerization from **3** to **4** the carbon atom migrates back from Mn to Re. Since the selective formation of M−C bonds is of great importance in the understanding of the reactivity of heterobimetallic systems, this peculiar behavior merits some discussion. We have previously pointed out that the cleavage of the S−C bond in the related homonuclear dimanganese and dirhenium complexes can be envisaged as an intramolecular oxidative addition within the anionic species resulting from the reduction of **1**.[3] Two possible paths for this process are depicted in Scheme 2. In path P(I), the migration of the carbon atom from Mn to Re would occur before the oxidative addition to give **B**, in which the carbon of the S$_2$CPR$_3$ ligand is bonded to Re. Subsequent addition of one C−S bond to Re produces **C**, which, after protonation, gives species **E**, where the electron counting assigns only 16 electrons to Mn. Addition of ammonia affords the final product **3**. Alternatively, if path P(II) of Scheme 2 is followed, the oxidative addition occurs before any migration to afford species **D**, in which the carbon atom is still bonded to Mn. The migration would take place then to afford **C**, which, on protonation, gives **E** and the final product **3**. Due to the high reactivity of the solutions produced after the reduction and before the protonation, there is little information available about the species that are actually present in these solutions, and therefore there are no empirical data to directly support either path. A close inspection of the structures of **5a** and **6b** (Figures 1 and 2) reveals that none of them is sterically congested, and therefore there is no steric requirement to force the rearrangement. This means that the driving force should be of electronic nature. We have found in our previous studies that the central carbon of the S$_2$CPR$_3$ is able to migrate between different metal atoms to follow changes in the electron density distribution of the metals involved.[4] The same reasoning can be applied to rationalize the driving force behind the migration from Mn to Re. In fact, arguments can be drawn in support of both paths considered in Scheme 2. An interesting difference between the two paths is that path P(I) involves a migration of the S$_2$CPR$_3$ ligand, while in path P(II) it is the new thiocarbonylphosphorane ligand, SCPR$_3$, that actually migrates. While the ability to migrate is well established for S$_2$CPR$_3$, the only precedent for SCPR$_3$ has been found recently in complex [Ni$_2$Cl$_2$(PMe$_3$)$_2$(μ-SCPMe$_3$)],[5]

(4) Miguel, D.; Pérez-Martínez, J. A.; Riera, V.; García-Granda, S. *Organometallics* **1994**, *13*, 4667.

(5) Klein, H. F.; Schmidt, A.; Flörke, U.; Haupt, H. J. *Angew Chem., Int. Ed.* **1998**, *37*, 2387.

Scheme 2

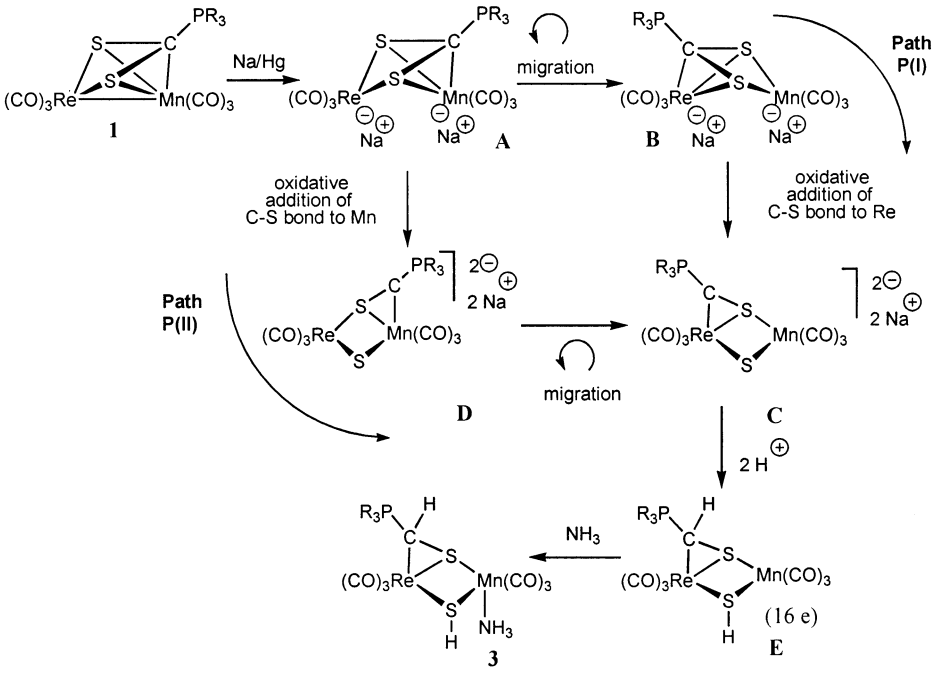

Scheme 3

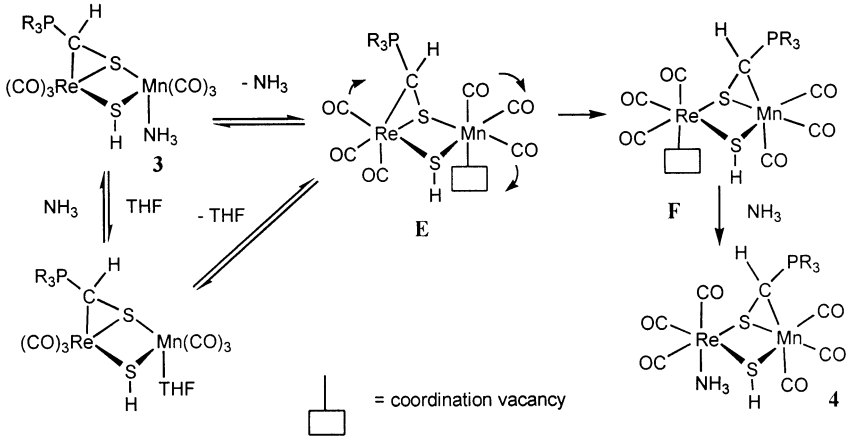

and no migration process has ever been described for this ligand.

The subsequent isomerization from **3** to **4** reveals that, in the protonated species the more stable isomer is **4**, containing the carbon atom of $SC(H)PR_3$ bonded to Mn. Hence, the first migration from Mn to Re must take place *before* the protonation. Thus, the anionic species **C**, obtained by either path P(I) or P(II) is probably the one that originates the IR spectra recorded for complexes **2** in the Experimental Section. Protonation with NH_4PF_6 gives **E**, and further coordination of NH_3 gives unstable compounds **3**, which spontaneously isomerize to **4**, as described above.

All experimental data available indicate that complexes **3** are able to dissociate NH_3 reversibly, thus regenerating the coordinatively unsaturated species **E** (see Scheme 3). When the solvent is a moderately good donor, such as THF, or there is excess NH_3, the migration is slowed. If the position is blocked by a good, nonlabile ligand (PEt_3 or $CNBu^t$) as in complexes **5a**−**d**, the isomerization is completely stopped. On the other hand, if no excess of NH_3 is present and the solvent is noncoordinating (CH_2Cl_2), the isomerization proceeds rapidly. The same occurs if THF and NH_3 are eliminated when the solution is evaporated to dryness.

Apart from the previously reported homobinuclear analogues,[3] the only precedent for the ligands $SC(H)PR_3$ had been found in the mononuclear complex [3-{η^2-$SC(H)PPh_3$}-3-(PPh_3)-*closo*-3,1,2-$RhC_2B_9H_{11}$].[6] As for $SCPR_3$, no migration process has been observed before for $SC(H)PR_3$.

Experimental Section

All reactions were carried out in dry solvents under a nitrogen atmosphere. Details of the instrumentation and experimental procedures have been given elsewhere.[7] Literature procedures for the preparation of starting materials are quoted in each case. Ligands and other reagents were purchased and used without purification unless otherwise stated.

(6) Ferguson, G.; Gallagher, J. F.; Jennings, M. C.; Coughlan, S.; Spalding, T. R.; Kennedy, J. D.; Fontaine, X. L. R. *J. Chem. Soc., Chem. Commun.* **1994**, 1595.

(7) Barrado, G.; Hricko, M. M.; Miguel, D.; Riera, V.; Wally, H.; García-Granda, S. *Organometallics* **1998**, *17*, 820.

$Na_2[MnRe(CO)_6(\mu\text{-}S_2CPCy_3)]$ (2a) in THF Solution. $[MnRe(CO)_6(\mu\text{-}S_2CPCy_3)]$ (**1a**) (0.10 g, 0.13 mmol) was dissolved in THF (20 mL), and the solution was cooled in an ice bath. Freshly prepared sodium amalgam (1% w/w, 10 g, excess) was then added, and the mixture was stirred for 15 min, when the IR spectrum of the solution showed that all starting **1a** had been consumed. The mixture was allowed to decant, and the solution was filtered through a cannula over the appropriate reagent to obtain the protonated derivatives **3a**. IR (THF): ν(CO) 1993m, 1957vs, 1876m, 1868s, cm^{-1}.

$Na_2[MnRe(CO)_6(\mu\text{-}S_2CPPr^i_3)]$ (2b) in THF Solution. The procedure was similar to that described above for the preparation of **2a**, starting from $[MnRe(CO)_6(\mu\text{-}S_2CPPr^i_3)]$ (**1b**) (0.12 g, 0.18 mmol) and sodium amalgam (1% w/w, 10 g, excess) in THF (10 mL). The reaction was completed in 15 min, and the solution was similarly filtered through a cannula to be used in subsequent reactions. IR (THF): ν(CO) 1994m, 1959vs, 1880m, 1869s, cm^{-1}.

$[MnRe(CO)_6(\mu\text{-}SH)\{\mu\text{-}SC(H)PCy_3\}(NH_3)]$ (3a). A solution of **2a** (0.13 mmol) in THF (20 mL), prepared as described above, was cooled to 0 °C and was transferred through a cannula into a Schlenck flask containing NH_4PF_6 (0.043 g, 0.26 mmol). The reaction was clean and instantaneous, according to IR monitoring, to give **3a**. On standing at room temperature or upon evaporation, compound **3a** isomerizes to **4a**. Therefore it could not be isolated for further characterization. However, the solution of **3a** can be used to prepare derivatives **5a** and **5c** through displacement of NH_3 by other ligands (see below). Data for **3a**: IR (THF) ν(CO) 2012m, 1985vs, 1909s, 1899s, 1881s, 1864s, cm^{-1}.

$[MnRe(CO)_6(\mu\text{-}SH)\{\mu\text{-}SC(H)PPr^i_3\}(NH_3)]$ (3b). A solution of **2b** (0.18 mmol) in THF (10 mL), prepared as described above, was cooled to 0 °C and was transferred through a cannula into a Schlenck flask containing NH_4PF_6 (0.059 g, 0.36 mmol). Similarly to **3a**, compound **3b** could not be isolated and was used in solution to prepare derivatives **5b** and **5d** (see below). Data for **3b**: IR (THF) ν(CO) 2013m, 1987vs, 1909s, 1901s, 1883s, 1866s, cm^{-1}.

$[MnRe(CO)_6(\mu\text{-}SH)\{\mu\text{-}SC(H)PCy_3\}(NH_3)]$ (4a). A solution of **3a** (0.13 mmol) prepared as described above was stirred at room temperature for 10 min. The solvent was evaporated in vacuo, and the residue was dissolved in a mixture of THF and hexane (1:1) and filtered through a short column (2.5 × 10 cm) of alumina (activation degree III). Evaporation of the solvent gave a yellow microcrystalline solid, which can be kept under nitrogen in a refrigerator for weeks, but decomposed in solution after several hours at room temperature. Yield: 0.062 g, 61% with respect to starting **1a**. Anal. Calcd for $C_{25}H_{38}MnNO_6PReS_2$: C, 38.26; H, 4.81; N, 1.78. Found: C, 38.53; H, 4.55; N, 1.58. IR (THF): ν(CO) 2011m, 1978s, 1889 vs, 1865s, cm^{-1}. ^1H NMR (THF-d_8): δ 2.84 [s, 3H, NH_3], 2.82 [s, 1H, SC(*H*)P)], 2.61−1.28 [m, 33 H, *Cy*], −2.08 [s, 1H, S*H*]. $^{31}P\{^1H\}$ NMR (THF-d_8): δ 44.8 [s, SC*P*]. $^{13}C\{^1H\}$ NMR (THF-d_8): 228.6, 224.2 [Mn*C*O], 197.9, 192.8, 192.2 [Re*C*O], 35.1 [d (43), C^1 of Cy)], 29.8 [d(40), S*C*(H)P], 28.0 [d(3)] and 27.9 [d(3)] [C^2 and C^6 of Cy], 27.8 d(12) and 27.4 d(11) (C^3 and C^5 of Cy), 26.5 (s, C^4 of Cy).

$[MnRe(CO)_6(\mu\text{-}SH)\{\mu\text{-}SC(H)PPr^i_3\}(NH_3)]$ (4b). Compound **4b** was prepared as described above for **4a**, from a solution of **3b** (0.18 mmol). The workup was as described for **4a** to afford **4b** as yellow microcrystals. Yield: 0.060 g, 50%. Anal. Calcd for $C_{16}H_{26}MnNO_6PReS_2$: C, 28.92; H, 3.94; N, 2.11. Found: C, 28.65; H, 4.21; N, 1.87. IR (THF): ν(CO) 2012m, 1980s, 1890vs, 1868s, cm^{-1}. ^1H NMR (CD_2Cl_2): δ 3.30 [s, 3H, NH_3], 2.79 [s, 1H, SC(*H*)P)], 2.58 [m, 3 H, C*H* of Pr^i], 1.49 [m, 18H, CH_3 of Pr^i], −2.34 [s, 1H, S*H*]. $^{31}P\{^1H\}$ NMR (CD_2Cl_2): δ 50.3 [s, SC*P*]. $^{13}C\{^1H\}$ NMR (CD_2Cl_2): 228.6, 227.8, 222.2 [Mn*C*O], 196.9, 193.9, 191.8 [Re*C*O], 24.9 [d(44), *C*H of Pr^i], 21.6 [d(42), S*C*(H)P], 18.6 [d(18), *C*H_3 of Pr^i].

$[MnRe(CO)_6(\mu\text{-}SH)\{\mu\text{-}SC(H)PCy_3\}(PEt_3)]$ (5a). To a cooled (−78 °C) solution of **3a** (0.13 mmol) prepared as described above was added PEt_3 (18 μL, 0.13 mmol), and the mixture was stirred for 30 min and was left to warm to room temperature. The solvent was evaporated in vacuo, the residue was extracted with CH_2Cl_2/hexane (1:4, v/v, 4 × 15 mL), and the collected extracts were filtered through a short column of alumina (2.5 × 5 cm, activation degree III). Slow concentration in vacuo afforded **5a** as a yellow microcrystalline solid. Yield: 0.061 g, 53%. Anal. Calcd for $C_{31}H_{50}MnO_6P_2ReS_2$: C, 42.03; H, 5.69. Found: C, 42.32; H, 5.58. IR (THF): ν(CO) 2006m, 1985vs, 1914s, 1905s, 1882s, 1866s, cm^{-1}. ^1H NMR (CD_2Cl_2): δ 2.68 [s, 1H, SC(*H*)P], 2.43−1.13 [m, 48H, *Cy* and *Et*], −1.97 [d(16), 1H, S*H*]. $^{31}P\{^1H\}$ NMR (CD_2Cl_2): δ 36.3 [s, SC*P*], 37.1 [s, *P*Et_3]. $^{13}C\{^1H\}$ NMR (CD_2Cl_2): 220.0, 218.1, 217.6 [3 × Mn*C*O], 200.1, 199.0, 194.8 [3 × Re*C*O], 33.5 [d (43), C^1 of Cy)], 26.9 d(2) and 26.6 d(2) (C^2 and C^6 of Cy), 26.3 d(12) and 25.8 d(11) (C^3 and C^5 of Cy), 25.0 (s, C^4 of Cy), 20.5 [dd(37 and 5), S*C*(H)P], 15.9 [d(22), *C*H_2 of PEt_3], 7.1 [s, *C*H_3 of PEt_3].

$[MnRe(CO)_6(\mu\text{-}SH)\{\mu\text{-}SC(H)PPr^i_3\}(PEt_3)]$ (5b). Compound **5b** was prepared as described above for **5a**, from a solution of **3b** (0.18 mmol) and PEt_3 (25 μL, 0.18 mmol). Yield: 0.1 g, 72%. Anal. Calcd for $C_{22}H_{38}MnO_6P_2ReS_2$: C, 34.51; H, 5.00. Found: C, 34.37; H, 5.23. IR (THF): ν(CO) 2007m, 1987vs, 1916s, 1904s, 1883s, 1867s, cm^{-1}. ^1H NMR ($CDCl_3$): δ 2.73 [s, 1H, SC(*H*)P], 2.55 [m, 3H, C*H* of Pr^i], 2.32 [m, 6H, CH_2 of Et], 1.56 [m, 18H, CH_3 of Pr^i], 1.24 [m, 9H, CH_3 of Et], −2.03 [d(16), 1H, S*H*]. $^{31}P\{^1H\}$ NMR ($CDCl_3$): δ 45.5 [s, SC*P*], 37.4 [s, *P*Et_3]. $^{13}C\{^1H\}$ NMR ($CDCl_3$): 220.8, 218.9 [3 × Mn*C*O], 200.5, 199.1, 195.7 [3 x Re*C*O], 24.5 [d (45), *C*H of Pr^i)], 18.3 [dd(42 and 6), S*C*(H)P], 18.0 [d(16), *C*H_3 of Pr^i], 16.7 [d(22), *C*H_2 of PEt_3], 8.1 [s, *C*H_3 of PEt_3].

$[MnRe(CO)_6(\mu\text{-}SH)\{\mu\text{-}SC(H)PCy_3\}(CNBu^t)]$ (5c). To a solution of **3a** (0.22 mmol) prepared as described above was added $CNBu^t$ (24 μL, 0.22 mmol), and the mixture was stirred for 10 min. The solvent was evaporated in vacuo, the residue was extracted with CH_2Cl_2/hexane (1:2, v/v, 3 × 15 mL), and the collected extracts were filtered through a short column of alumina (2.5 × 5 cm, activation degree III). Slow concentration in vacuo afforded **5c** as a yellow microcrystalline solid. Yield: 0.085 g, 44%. Anal. Calcd for $C_{30}H_{44}MnNO_6PReS_2$: C, 42.34; H, 5.21; N, 1.64. Found: C, 42.30; H, 5.35; N, 1.88. IR (THF): ν(CN) 2171 s, cm^{-1}; ν(CO) 2016m, 1988vs, 1935w, 1927m, 1883s, 1864s, cm^{-1}. ^1H NMR (CD_2Cl_2): δ 2.37 [s, 1H, SC(*H*)P], 2.37−1.36 [m, 42H, *Cy* and *Bu*^{t}], −2.15 [s, 1H, S*H*]. $^{31}P\{^1H\}$ NMR (CD_2Cl_2): δ 36.6 [s, SC*P*]. $^{13}C\{^1H\}$ NMR (CD_2Cl_2): 220.2, 218.2, 217.0 [3 × Mn*C*O], 202.2, 199.9, 196.4 [3 × Re*C*O], 163.0 [s, *C*NBu^t], 59.0 [s, CN*C*Me_3], 34.5 [d (43), C^1 of Cy)], 30.7 [s, *C*H_3 of Bu^t], 28.2 d(3) and 26.6 d(2) (C^2 and C^6 of Cy), 27.4 d(11) and 26.9 d(11) (C^3 and C^5 of Cy), 26.1 (s, C^4 of Cy), 19.4 [d(35), S*C*(H)P].

$[MnRe(CO)_6(\mu\text{-}SH)\{\mu\text{-}SC(H)PPr^i_3\}(CNBu^t)]$ (5d). Compound **5d** was prepared as described above for **5c** starting from a solution of **3b** (0.14 mmol) and $CNBu^t$ (15 μL, 0.14 mmol). After stirring for 5 min, the solvent was evaporated in vacuo, the residue was extracted with CH_2Cl_2/hexane (1:1, v/v, 3 × 15 mL), and the collected extracts were filtered through a short column of alumina (2.5 × 5 cm, activation degree III). Slow concentration in vacuo afforded **5d** as a yellow microcrystalline solid. Yield: 0.065 g, 64%. Anal. Calcd for $C_{21}H_{32}MnNO_6PReS_2$: C, 34.51; H, 4.41; N, 1.91. Found: C, 34.27; H, 4.56; N, 1.88. IR (THF): ν(CN) 2171 s, cm^{-1}; ν(CO) 2017m, 1989vs, 1939w, 1927s, 1885vs, 1866s, cm^{-1}. ^1H NMR ($CDCl_3$): δ 2.53 [m, 3H, C*H* of Pr^i], 2.37 [s, 1H, SC(*H*)P], 1.66 [s, 9H, CH_3 of $CNBu^t$], 1.46 [m, 18H, CH_3 of Pr^i], −2.03 [s, 1H, S*H*]. $^{31}P\{^1H\}$ NMR (CD_2Cl_2) δ 45.8 [s, SC*P*]. $^{13}C\{^1H\}$ NMR (CD_2Cl_2): 220.3, 217.4, 216.5 [3 × Mn*C*O], 202.4, 199.9, 196.8 [3 × Re*C*O], 163.0 [s, *C*NBu^t], 59.3 [s, CN*C*Me_3], 31.1 [s, *C*H_3 of Bu^t], 25.0 [d (45), *C*H of Pr^i)], 18.0 [d(17), *C*H_3 of Pr^i], 17.2 [d(36), S*C*(H)P].

$[MnRe(CO)_6(\mu\text{-}SH)\{\mu\text{-}SC(H)PCy_3\}(PEt_3)]$ (6a). To a solution of **3b** (0.26 mmol) prepared as described above was added PEt_3 (36 μL, 0.26 mmol), and the mixture was stirred for 30 min at 40 °C. The solvent was evaporated in vacuo, the residue

was extracted with CH_2Cl_2/hexane (1:1, v/v, 4 × 10 mL), and the collected extracts were filtered through a short column of alumina (2.5 × 5 cm, activation degree III). Slow concentration in vacuo afforded **6a** as a yellow microcrystalline solid. Yield: 0.150 g, 65%. Anal. Calcd for $C_{31}H_{50}MnO_6P_2ReS_2$: C, 42.03; H, 5.69. Found: C, 42.14; H, 5.85. IR (THF): ν(CO) 2011m, 1979s, 1911m, 1891s, 1885s, 1869m, cm^{-1}. ^1H NMR (CD_2Cl_2): δ 3.05 [s, 1H, SC(*H*)P], 2.45−1.12 [m, 48H, *Cy* and *Et*], −2.15 [d(14), 1H, S*H*]. $^{31}P\{^1H\}$ NMR (CD_2Cl_2): δ 40.5 [s, SC*P*], −0.33 [s, *P*Et_3]. $^{13}C\{^1H\}$ NMR (CD_2Cl_2): 231.2, 229.8, 229.5 [3 × Mn*C*O], 194.5, 190.7, 189.9 [3 × Re*C*O], 33.5 [d (42), C^1 of Cy)], 31.9 [dd(42 and 5), S*C*(H)P], 26.7 d(4) and 26.3 d(6) (C^2 and C^6 of Cy), 25.9 d(12) and 25.7 d(11) (C^3 and C^5 of Cy), 24.7 (s, C^4 of Cy), 15.6 [d(27), *C*H_2 of PEt_3], 7.0 [s, *C*H_3 of PEt_3].

[MnRe(CO)$_6$(μ-SH){μ-SC(H)PPr$^i_3$}(PEt$_3$)] (6b). A solution of **4b** (0.23 mmol) and PEt_3 (31 μL, 0.23 mmol) in THF (25 mL) was stirred for 30 min at 40 °C, and then the solvent was evaporated in vacuo. The residue was dissolved in CH_2Cl_2/hexane (1:3, v/v) and filtered through alumina. Subsequent evaporation gave **6b** as a yellow microcrystalline solid. Yield: 0.114 g, 69%. Anal. Calcd for $C_{22}H_{38}MnO_6P_2ReS_2$: C, 34.51; H, 5.00. Found: C, 34.30; H, 5.13. IR (THF): ν(CO) 2012m, 1981vs, 1913s, 1892(sh), 1888s, 1870m, cm^{-1}. ^1H NMR ($CDCl_3$): δ 2.96 [d(2), 1H, SC(*H*)P], 2.57 [m, 3H, C*H* of Pr^i], 2.37 [m, 6H, CH_2 of Et], 1.57 [m, 18H, CH_3 of Pr^i], 1.18 [m, 9H, CH_3 of Et], −2.19 [d(13), 1H, S*H*]. $^{31}P\{^1H\}$ NMR ($CDCl_3$): δ 49.8 [s, SC*P*], −0.23 [s, *P*Et_3]. $^{13}C\{^1H\}$ NMR (CD_2Cl_2): 228.7, 226.4, 223.3 [3 × Mn*C*O], 195.5, 194.7 [2 × Re*C*O], 191.7 [dd(43 and 7), Re*C*O], 31.1 [dd(41 and 5), S*C*(H)P], 24.8 [d (44), *C*H of Pr^i)], 18.1 [dd(16 and 3), *C*H_3 of Pr^i], 16.9 [d(28), *C*H_2 of PEt_3], 8.1 [s, *C*H_3 of PEt_3].

[MnRe(CO)$_6$(μ-SH){μ-SC(H)PCy$_3$}(CNBu^t)] (6c). A solution of **4a** (0.13 mmol) and CNBu^t (14 μL, 0.13 mmol) in THF (20 mL) was stirred for 1 h at 40 °C. The workup was as described above for **6a** to afford yellow microcystals of **6b**. Yield: 0.050 g, 50%. Anal. Calcd for $C_{30}H_{44}MnNO_6PReS_2$: C, 42.34; H, 5.21; N, 1.64. Found: C, 42.41; H, 5.37; N, 1.79. IR (THF): ν(CN) 2179 s, cm^{-1}; ν (CO) 2015m, 1982vs, 1929s, 1911s, 1888s, 1868s, cm^{-1}. ^1H NMR (CD_2Cl_2): δ 2.66 [s, 1H, SC(*H*)P], 2.36−1.34 [m, 42H, *Cy* and *Bu^t*], −2.34 [s, 1H, S*H*]. $^{31}P\{^1H\}$ NMR (CD_2Cl_2): δ 40.4 [s, SC*P*]. $^{13}C\{^1H\}$ NMR (CD_2Cl_2): 228.4, 223.4 [3 × Mn*C*O], 194.4, 188.9, 188.7 [3 × Re*C*O], 139.2 [s, *C*NBu^t], 59.2 [s, CN*C*Me$_3$], 35.1 [d (44), C^1 of Cy)], 31.2 [d(39), S*C*(H)P], 31.1 [s, *C*H_3 of Bu^t], 28.6 d(4) and 28.1 d(3) (C^2 and C^6 of Cy), 27.8 d(10) and 27.4 d(12) (C^3 and C^5 of Cy), 26.5 (s, C^4 of Cy).

[MnRe(CO)$_6$(μ-SH){μ-SC(H)PPr$^i_3$}(CNBu^t)] (6d). Compound **6d** was prepared as described above for **6a** starting from a solution of **4b** (0.15 mmol) and CNBu^t (17 μL, 0.15 mmol). After stirring for 30 min, the solvent was evaporated in vacuo, the residue was extracted with CH_2Cl_2/hexane (1:1, v/v, 3 × 15 mL), and the collected extracts were filtered through alumina. Slow concentration in vacuo afforded **6d** as a yellow microcrystalline solid. Yield: 0.052 g, 48%. Anal. Calcd for $C_{21}H_{32}MnNO_6PReS_2$: C, 34.51; H, 4.41; N, 1.91. Found: C, 34.27; H, 4.56; N, 1.88. IR (THF): ν(CN) 2171 s, cm^{-1}; ν(CO) 2015s, 1983vs, 1931s, 1911s, 1889s, 1869s, cm^{-1}. ^1H NMR (CD_2Cl_2): δ 2.71 [s, 1H, SC(*H*)P], 2.66 [m, 3H, C*H* of Pr^i], 1.74 [s, 9H, CH_3 of CNBu^t], 1.53 [m, 18H, CH_3 of Pr^i], −2.31 [s, 1H, S*H*]. $^{31}P\{^1H\}$ NMR (CD_2Cl_2): δ 49.8 [s, SC*P*]. $^{13}C\{^1H\}$ NMR (CD_2Cl_2): 228.4, 224.2 [3 × Mn*C*O], 194.7, 188.9, 188.5 [3 × Re*C*O], 139.2 [s, *C*NBu^t], 59.3 [s, CN*C*Me$_3$], 30.9 [s, *C*H_3 of Bu^t], 28.7 [d(40), S*C*(H)P], 25.0 [d (45), *C*H of Pr^i)], 18.6 [d(19), *C*H_3 of Pr^i].

[MnRe(CO)$_6$(μ-SH){μ-SC(H)PCy$_3$}(PPh$_3$)] (6e). A solution of **3b** (0.11 mmol) and PPh_3 (0.033 g, 0.11 mmol) in THF (20 mL) was stirred for 90 min at 40 °C. The solvent was evaporated in vacuo, the residue was extracted with CH_2Cl_2/hexane (1:1, v/v, 4 × 10 mL), and the collected extracts were filtered through alumina. Slow concentration in vacuo afforded **6e** as yellow microcrystals. Yield: 0.055 g, 44%. Anal. Calcd for $C_{43}H_{50}MnO_6P_2ReS_2$: C, 50.14; H, 4.89. Found: C, 49.98; H, 5.06. IR (THF): ν(CO) 2013m, 1982s, 1917m, 1901s, 1890vs, 1868m, cm^{-1}. ^1H NMR (CD_2Cl_2): δ 7.79−7.45 [m, 15H, PC_6H_5], 3.09 [s, 1H, SC(*H*)P], 2.43−0.85 [m, 33H, *Cy*], −2.01 [d(11), 1H, S*H*]. $^{31}P\{^1H\}$ NMR ($CDCl_3$): δ 41.2 [s, SC*P*], 14.7 [s, *P*Ph_3]. $^{13}C\{^1H\}$ NMR (CD_2Cl_2): 229.6, 224.5, 223.4 [3 × Mn*C*O], 195.2, 194.4, 191.7 [3 × Re*C*O], 134.7 [d(11), C^3 and C^5 of Ph], 132.9 [d(44), C^1 of Ph], 130.6 [d(2), C^4], 128.6 [d(10), C^2 and C^6 of Ph], 34.6 [d(43), C^1 of Cy)], 32.2 [dd(42 and 6), S*C*(H)P], 28.2 d(4) and 27.6 d(4) (C^2 and C^6 of Cy), 27.5 d(11) and 27.0 d(11) (C^3 and C^5 of Cy), 26.1 (s, C^4 of Cy).

X-ray Diffraction Study of 5a and 6d. Crystals were grown by slow difusion of hexane into a concentrated solutions of the complexes in THF at −20 °C. Relevant crystallographic details are given in Table 1. Unit cell parameters were determined from the least-squares refinement of a set of 25 centered reflections in the range $15 < \theta < 18$. Three reflections were measured every 1 h as orientation and intensity control. Significant decay was not observed. The structures were solved by Patterson methods, phase expansion, and subsequent Fourier maps with DIRDIF.[8] Full-matrix least-squares refinement was made with SHELX-93.[9] All non-hydrogen atoms were refined anisotropically. Hydrogen atoms were geometrically positioned, with a common isotropic temperature factor, which was refined. Perspective drawing in Figures 1 and 2 were made with PLATON.[10]

Acknowledgment. We thank the Spanish Dirección General de Investigación Científica y Técnica (Projects PB97 0470-C02-01 and BQU2000-0219) for financial support. We also thank CICYT for a grant to J.L.

Supporting Information Available: Complete tables of atomic coordinates, anisotropic thermal parameters, and bond lengths and angles for the structures of **5a** and **6d**. This material is available free of charge via the Internet at http://pubs.acs.org. Lists of structure factor amplitudes are available from the authors.

OM0100232

(8) Beurskens, P. T.; Admiraal, G.; Bosman, W. P.; Beurskens, G.; Doesburg, H. M.; García-Granda, S.; Gould, R. O.; Smits, J. M. M.; Smikalla, C. *The DIRDIF Program System, Technical Report of the Crystallography Laboratory*; University of Nijmegen: The Netherlands, 1992.

(9) Sheldrick, G. M. *SHELX-93*; University of Göttingen, 1993.

(10) Spek, A. L. The EUCLID Package. In *Computational Crystallography*; Sayre, E., Ed.; Clarendon Press: Oxford, England, 1982; p 528.